Domains of phase separation in a charged colloidal dispersion driven by electrolytes

G. F. Wang and S. K. Lai*

Complex Liquids Laboratory, Department of Physics, National Central University, Chungli 320, Taiwan, Republic of China

(Received 23 March 2004; revised manuscript received 6 July 2004; published 15 November 2004)

We put forth the idea of treating coexisting phases as a composite system and express its free energy as the average of its constitutent free energies weighted by their respective volume proportions. As a result, the theoretical study of charged colloidal phase separation in the presence of electrolytes reduces to optimizing solely the entities pertaining to colloids and small ions. As concrete illustrations, we demarcated the boundaries of coexisting phases for the simplest colloidal dispersion driven by salts at moderate to high concentrations and compared the results with those obtained in the usual manner to numerically show the robust efficiency of the present theory. Also, for a charged colloidal dispersion at very low ionic strength, we crosshatched both the homogeneous one phase and coexisting phases, and used the domains of coexisting phases to interpret an anomalous "transition" of phase diagrams exhibited in dilute colloidal dispersions induced by salts on dilution.

DOI: 10.1103/PhysRevE.70.051402 PACS number(s): 61.43.Hv, 05.70.Fh, 64.70.Ja, 82.70.Dd

I. INTRODUCTION

A deionized charged colloidal dispersion consists of macroions, oppositely charged counterions, and a dispersive medium throughout which these charged particles are immersed and distributed under the combined operation of their thermal motion and the electrostatic interactions among them. At a fixed temperature, it would be reasonable to expect the addition of an electrolyte to the system to be structurally and thermodynamically crucial since any variation in the salt concentration would noticeably affect the colloidal equilibrium behavior, resulting in most cases in drastic changes in the structure of the phase diagram. Figure 1(a) shows a phase diagram calculated for a low density colloidal dispersion. At an initial colloidal volume fraction $\eta_0 \approx 0.05$, it is seen that an increase in the initial salt concentration $\rho_0^{(s)}$ spanning over the range $0 < \rho_0^{(s)} < 180$ μM has the effect of inducing phase separation; the system displays first a vapor-crystal (fcc) which continues until in the vicinity of $\rho_0^{(s)} \approx 179$ μM, and then changes over to a liquid-crystal transition. When the colloidal charge is reduced to beyond a threshold value, keeping all other colloidal parameters unchanged, it is found below that the vapor-crystal transition disappears and the phase separation is characterized by the liquid-crystal transition only. These features are in marked contrast to the concentrated charged colloidal dispersions at appreciable amounts of electrolyte concentrations where now the electrostatic repulsion between colloids is considerably weakened and replaced by the gradually strengthened van der Waals attraction. Here experiments, computer simulations, and theories have been rather successful [1,2] in revealing consistent phase diagrams. Typical phase boundaries are displayed in Fig. 1(b) for the liquid-liquid and liquid-crystal transitions [3,4]. In view of these variant structures, an understanding of the charged colloidal phase equilibrium phenomena from very low salt concentration ($\lesssim 1$ μM) to moderate and high regimes (>1 mM) is thus a great challenge to both theorists and experimentalists.

Already, ample experimental works on charged colloidal suspensions have been reported in the literature. The aqueous dispersions of polystyrene latices, polymer latex particles, silica, etc., are few of the popular and well-studied types of colloids. Generally, the measured phase diagrams for these

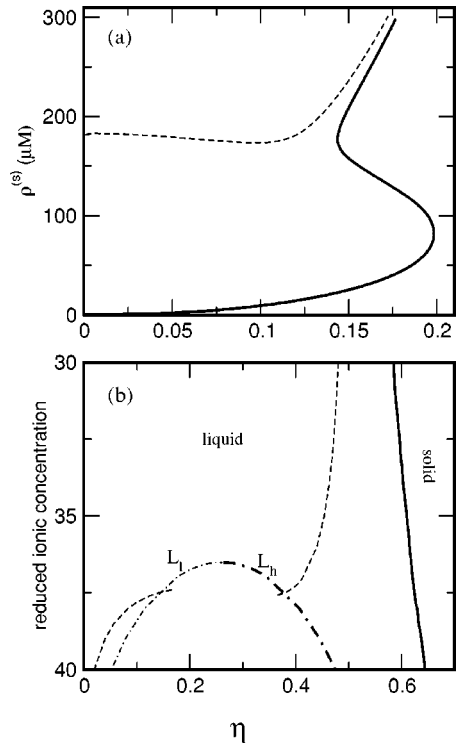

FIG. 1. Phase diagram for ionic strength $\rho^{(s)}$ vs volume fraction η of colloids for charge-stabilized colloidal dispersions induced at (a) low, $\rho_0^{(s)} \lesssim 1$ μM and (b) moderate to high, $\rho_0^{(s)} \gtrsim 1$ mM, concentration of electrolytes. Notations used are (a) dashed line, low density branch fluid (vapor or liquid); solid line, high density branch (fcc) solid; and (b) dashed line, low density branch fluid (vapor or liquid); solid line, high density (fcc) solid; light dot-dashed line, low density liquid labeled L_1; heavy dot-dashed line, high density liquid labeled L_h.

*Electronic address: sklai@cliq.phy.ncu.edu.tw

systems at higher $\rho_0^{(s)}(>1\ \mathrm{mM})$ were convincingly interpreted [4], although some often raised issue of concern in globular proteins (e.g., the mechanism of crystallization phenomena) remains to be understood. In contrast, many of the experimental results for lyophobic colloids at dilute salt concentrations are, however, unexplained, unsatisfactorily understood, or have aroused controversial in interpretation.

Turning to theories, related quantitative models [5,6] at a microscopic level have only very recently appeared in the literature. These theoretical efforts generally fall into two categories. The first category considers the possibility of the existence of attractive forces between colloidal particles in addition to the well known Derjaguin-Landau-Verwey-Overbeek [7] repulsive interaction. With the introduction of the former contribution, an effective two-body colloid-colloid potential is constructed, and in conjunction with a computer simulation technique is applied to study the phase transition of colloidal dispersions [8]. The presence of an attractive interaction in charged colloids has been an issue of controversy, however. The second category emphasizes the importance of the so-called volume terms in the free energy function [5,9,10] which is constructed from the well-established liquid-state theory in conjunction with the density functional method. The emergence of the negative energy contribution in volume terms has been identified as an important source for understanding the phase transition and is of much relevance to the theory presented below. Surprisingly, the rigorous theories in this category have so far not been checked quantitatively against experiments. On the other hand, the theoretical efforts in the first category have been used to interpret structural anomalies manifested in dilute ionic colloidal dispersions. The situation here is that it was reported earlier by Matsuoka *et al.* [11] and more recently by Yamanaka *et al.* [12] that the presence of very low salt concentrations in a system of dilute polystyrene latices (silica) has an immediate consequence; the nearest neighbor distance first increases (decreases) and the increment (decrement) continues until it reaches a maximum (minimum) distance. The interesting feature is, that with further addition of salt, the distance is observed to decrease (increase). The theoretical interpretation of this curious behavior within the theoretical framework in the first category was generally unsatisfactory. In this work, we propose a different means to study the phase separation. As we will see below, the theory is strategically elegant since it can be applied to charged colloidal dispersions induced at *any* salt concentration. More importantly, the calculation appeals to the free energy function only, which can be handled more straightforwardly than calculating the free energy function differentiation to obtain the pressure and chemical potential. Furthermore, the theory yields the domains of homogeneous *single phase* and *phases in coexistence* in addition to demarcating the phase boundaries of coexisting phases. Since colloidal experiments start with a given initial number density ρ_0 of colloids where $\rho_0 = 6\eta_0/(\pi\sigma^3)$, η_0 and σ being the volume fraction and particle diameter, respectively, monitoring its behavior by changing the control parameter $\rho_0^{(s)}$ or temperature, the present approach mimics closely the experimental condition.

II. THEORY

In this section, the general theory for calculating the domains of phase separation is first presented. Then we give essential equations needed in the numerical work. Since detailed expressions have been well documented in the literature, we shall be brief in our description of the latter.

A. Helmholtz free energy: General

Consider a homogeneous charged colloidal system of total volume V in which are contained N_0 charged colloids and $N_0^{(s)}$ small ions (counterions and coions); the total number densities of colloids and small ions are $\rho_0 = N_0/V$ and $\rho_0^{(s)} = N_0^{(s)}/V$, respectively. Suppose under favorable conditions the colloidal system phase-separates into two coexisting subsystems. Let us assume that V_i, $i=1$, 2, are the volumes of the subsystems and that inside V_i are contained N_i colloids plus $N_i^{(s)}$ small ions; the corresponding number densities are $\rho_i = N_i/V_i$ and $\rho_i^{(s)} = N_i^{(s)}/V_i$, respectively. Note that the subscripts $i=1$ and 2 refer to phase-separated subsystems in which are contained colloids of the *same* species. We label by $x_i = V_i/V$ the volume fraction of the ith subsystem and assume, in undergoing phase separation, that the system "composite" free energy density reads

$$f_m(\rho_1, \rho_1^{(s)}; \rho_2, \rho_2^{(s)}) = x_1 f_1(\rho_1, \rho_1^{(s)}) + x_2 f_2(\rho_2, \rho_2^{(s)}), \qquad (1)$$

where f_i is the ith subsystem free energy density which can be a function describing a solid, liquid, or gas depending on the thermodynamic equilibrium conditions. Now, if the combined effects of the electrostatic interaction and thermal equilibrium factor were to induce phase separation in the colloidal dispersion, in that case the homogeneous system decomposes into $f_1(\rho_1, \rho_1^{(s)})$ and $f_2(\rho_2, \rho_2^{(s)})$, and f_m given by Eq. (1) must have a lower free energy density than f_1 and f_2 separately evaluated at the homogeneous number densities ρ_0 and $\rho_0^{(s)}$. Since $x_1 + x_2 = 1$, $N_1 + N_2 = N_0$, and $N_1^{(s)} + N_2^{(s)} = N_0^{(s)}$, the subsystems x_i can be written as either $x_1 = (\rho_0 - \rho_2)/(\rho_1 - \rho_2)$ and $x_2 = -(\rho_0 - \rho_1)/(\rho_1 - \rho_2)$, or by the charge neutrality constraint, $x_1 = (\rho_0^{(s)} - \rho_2^{(s)})/(\rho_1^{(s)} - \rho_2^{(s)})$ and $x_2 = -(\rho_0^{(s)} - \rho_1^{(s)})/(\rho_1^{(s)} - \rho_2^{(s)})$. In order that f_m achieves the lowest free energy, we require

$$\left(\frac{\partial f_m}{\partial \rho_1}\right)_{\rho_2, \rho_1^{(s)}, \rho_2^{(s)}} = 0, \qquad (2)$$

$$\left(\frac{\partial f_m}{\partial \rho_2}\right)_{\rho_1, \rho_1^{(s)}, \rho_2^{(s)}} = 0, \qquad (3)$$

$$\left(\frac{\partial f_m}{\partial \rho_1^{(s)}}\right)_{\rho_1, \rho_2, \rho_2^{(s)}} = 0, \qquad (4)$$

$$\left(\frac{\partial f_m}{\partial \rho_2^{(s)}}\right)_{\rho_1, \rho_2, \rho_1^{(s)}} = 0, \qquad (5)$$

subject to the conditions of the conservation of volume and number of particles. Equations (1)–(5) in conjunction with

$x_1+x_2=1$, $x_1\rho_1+x_2\rho_2=\rho_0$, and $x_1\rho_1^{(s)}+x_2\rho_2^{(s)}=\rho_0^{(s)}$ can be shown by the method of Lagrangian multipliers [13] to lead to

$$\mu_1(\rho_1)=\mu_2(\rho_2), \tag{6}$$

$$\mu_1(\rho_1^{(s)})=\mu_2(\rho_2^{(s)}), \tag{7}$$

$$p_1(\rho_1,\rho_1^{(s)})=p_2(\rho_2,\rho_2^{(s)}), \tag{8}$$

which are three familiar conditions for the chemical potential μ_i and pressure p_i satisfied by two subsystems in coexistence [5]. Equations (6)–(8) are the necessary and sufficient conditions customarily used in the literature for determining the phase boundaries of two coexisting phases for a charge-stabilized colloidal dispersion at very low ionic strength. In the event that appreciable amounts of electrolyte are present in the system, $f_m(\rho_1,\rho_1^{(s)};\rho_2,\rho_2^{(s)})\approx f_m(\rho_1,\rho_0^{(s)};\rho_2,\rho_0^{(s)})$, only Eqs. (2) and (3) [and hence Eqs. (6) and (8) in which $\rho_1^{(s)}=\rho_2^{(s)}=\rho_0^{(s)}$] remain and we are led to the thermodynamic equilibrium conditions of constant chemical potential and pressure for colloids [4]. Thus, for a system of charged colloids with the addition of salts, one can crosshatch the *domains* (as well as the phase boundaries) of two coexisting phases by minimizing f_m defined by Eq. (1) only. Given ρ_0 and $\rho_0^{(s)}$ which are initial conditions for all experiments, Eqs. (1)–(5) can be used to extract $(\rho_1,\rho_1^{(s)};\rho_2,\rho_2^{(s)})$ and hence the phase diagram $\rho^{(s)}-\rho$. It is clear thus that in order to apply Eq. (1) the liquid and solid f_i under different $\rho_0^{(s)}$ environment are required. We turn next to a brief documentation of these functions.

B. Helmholtz free energy: $\rho_0^{(s)}\gtrsim 1$ mM

To study the phase transition of a charge-stabilized colloidal suspension for $\rho_0^{(s)}$ that falls in this range, we apply a full second-order perturbation equation to calculate the Helmholtz free energy density f_i, i=fluid or solid. According to our recent work [4], f_i can be written as

$$\beta f_i=\beta f_{\rm HS}(\eta)+12\eta_0^2\int_S^\infty dx\,x^2[\beta v_a(x)]g_{\rm HS}(x/S;\eta)-(6\eta_0^2/\beta)\times\left(\frac{\partial\rho}{\partial p_{\rm HS}(\eta)}\right)\int_S^\infty dx\,x^2[\beta v_a(x)]^2 g_{\rm HS}(x/S;\eta), \tag{9}$$

where $\beta f_{\rm HS}$ is the free energy density of hard spheres; S is the Barker-Henderson diameter; $v_a(x)$ is an attractive perturbation defined according to the Week-Chandler-Andersen method; $g_{\rm HS}(x/S;\eta)$ is the hard-sphere pair correlation function calculated at the effective η; $(1/\beta)(\partial\rho/\partial p_{\rm HS})=[1/(Z_{\rm HS}+\eta\partial Z_{\rm HS}/\partial\eta)]$ is the macroscopic compressibility in which $Z_{\rm HS}$ is the hard-sphere equation of state which reads differently for a liquid and a solid. All these quantities are well documented in Ref. [4] to which the interested readers are referred for further details.

C. Helmholtz free energy: $\rho_0^{(s)}\lesssim 1$ μM

For a charge-stabilized colloidal suspension at very low ionic strength, the Helmholtz free energy density can be shown to read [5,9,10]

$$f_i=f_{\text{st-GB}}+f_{\rm vol}, \tag{10}$$

where $f_{\text{st-GB}}=f^{(\rm id)}+f_{\rm GB}^{\rm ex}$ in which $f^{(\rm id)}$ and $f_{\rm GB}^{\rm ex}$ are, respectively, the ideal gas part and the excess interacting part of the free energy densities of colloids. Note that Eq. (10) was derived [9,10] by reducing first of all a total potential of two components (colloids plus small ions) to an effective one component within the Born-Oppenheimer approximation. The effective one-component total potential comprises two contributions. One contribution is the *structure-dependent* interacting potential which is used in $f_{\rm GB}^{\rm ex}$ and the other is the *state-dependent* $f_{\rm vol}$ in Eq. (10) which is the Helmholtz free energy of an inhomogeneous fluid of small ions calculated by treating the macroions as an external field at a given configuration. We have employed the widely used Gibbs Bogoliubov inequality [14] to calculate $f_{\rm GB}^{\rm ex}$. In doing so, the distribution function of the reference system is used to carry out the thermal average. For the reference system chosen in the variational calculation, we use the hard-sphere [14] and the Einstein crystalline [15] models to account for the liquid and solid phases, respectively. Also, density functional theory [16] has been applied to derive $f_{\rm vol}$. This so-called volume-term contribution is given by [5]

$$f_{\rm vol}=f_{+,-}^m+f_{\text{ex-}v}+f_{\rm elecst}. \tag{11}$$

In Eq. (11), $f_{+,-}^m$ is the ideal gas free energy contribution coming from the small ions (counterions, positive and negative ions); $f_{\text{ex-}v}$ is the contribution due to the excluded volume interactions of small ions within the finite-size colloids that occupy the "hard-sphere" volumes, and $f_{\rm elecst}$ is the negative energy terms arising from the electrostatic interactions between each structure-independent macroion and its surrounding clouds of small ions. Explicit expressions for all of these quantities are given in Ref. [5] to which the interested readers are referred.

III. NUMERICAL RESULTS AND DISCUSSION

To illustrate the distinctiveness of the theory, we first study the simplest two phases in coexistence. The system considered is an aqueous dispersion of monodisperse charged colloids. The size and surface potential of each colloid are 300 nm and 25 mV, respectively. For a concentrated charged colloidal dispersion driven by salts at moderate to high electrolyte concentrations (>1 mM), the colloid-colloid electrostatic repulsion is considerably weakened. In contrast, the colloid-colloid van der Waals attraction comes into play and its strength is governed by the Hamaker constant A which we fix at 8.3×10^{-20} J/K. Appealing to Eq. (9) for the liquid and solid free energy density functions, we optimize Eq. (1) for two selected colloidal densities ρ_0 or volume fractions $\eta_0=\pi\sigma^3\rho_0/6$, namely, $\eta_0=0.45$ and 0.25, and vary $\rho_0^{(s)}$ in the range $10^{-4}M<\rho_0^{(s)}<10^{-1}M$ (or the reduced parameter $29<\kappa=k_D\sigma\leqslant 45$ where k_D is the Debye screening

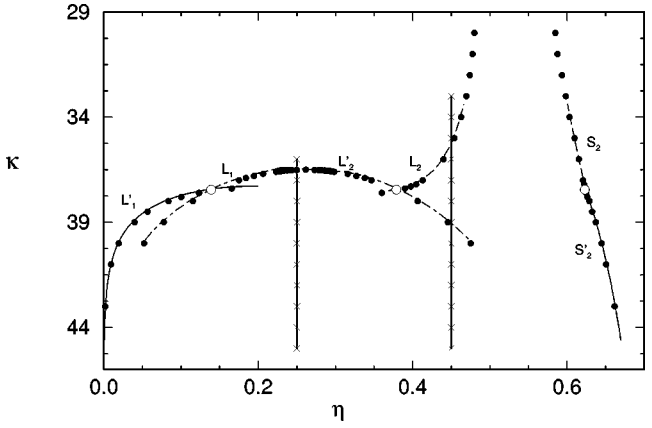

FIG. 2. Phase diagram for reduced ionic concentration κ vs packing ratio η for a charged colloidal dispersion at room temperature. $L_1, L_1', L_2, L_2', S_2'$, and S_2 are branches to be referred to in Fig. 3 (see text). Solid circles are results obtained as described in Ref. [4] compared with the present theory (full, dashed, and dot-dashed lines). The crosses on the two vertical full curves are initial densities of electrolytes and colloids (see text) and open circles are the liquid-liquid-solid triple points.

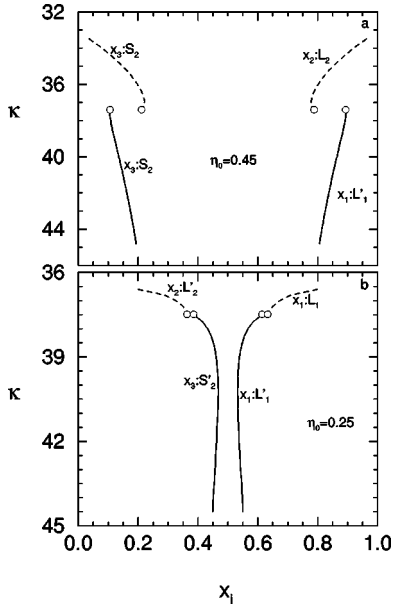

FIG. 3. Phase diagram for reduced ionic concentration κ vs volume proportion x_i [$i=1$, vapor; $i=2$, liquid; $i=3$, (fcc) solid] for a charged colloidal dispersion at room temperature. $L_1, L_1', L_2, L_2', S_2$, and S_2' are branches defined in Fig. 2. The label $x_i{:}L_j$ or $x_i{:}S_k$ means the volume proportion of phase i along the branch L_j or S_k. Open circles are the liquid-liquid-solid triple points defined in Fig. 2.

constant [4]). The calculated phase boundaries for the liquid-liquid and liquid-crystal (fcc) transitions are shown in Fig. 2. We should emphasize that, in optimizing f_m, we search and compare at each initial $(\rho_0^{(s)}, \rho_0)$ all possible phases: three single-phase (vapor, liquid, solid) and nine two-phase (vapor-vapor, vapor-liquid, vapor-solid, liquid-liquid, etc.) systems; the lowest f_m among these single and two coexisting phases is the one sought for. In Fig. 2 we compare the phase diagram which contains the liquid-liquid-solid triple points (open circles) with that calculated in our recent work (Fig. 1 of Ref. [4]) by solving Eqs. (6) and (8); the excellent agreement between the two results lends great credence to our recent work on one hand, but on the other hand, the fact that the same phase boundaries were reproduced demonstrates further the robust efficiency of the present theory to be strategically superior. Also, we depict in Fig. 3 the volume proportion x_i of each of the separated phases. We find that, for two phases to coexist, x_i and x_j have to change oppositely as $\rho_0^{(s)}$ increases at a given η_0. Let us scrutinize two cases in detail. Consider the first case $\eta_0=0.45$ given in Fig. 3(a). The solid phase x_3 (vapor phase x_1) decreases (increases) all the way from high κ till the proximity of $\kappa_{\rm tr}=37.4$, and for $\kappa<\kappa_{\rm tr}$ (refer also to Fig. 2), the vapor to low density liquid x_1 (L_1' branch) is replaced by the L_2 branch, being a higher density liquid characterized by the volume proportion x_2. This x_2 increases at the expense of the solid phase x_3 (S_2 branch). The situation for the second case $\eta_0=0.25$ [Fig. 3(b)] is opposite. Here, the solid phase x_3 (vapor phase x_1) first increases (decreases) slightly with decreasing κ, and these changes of x_i extend up to a common maximized (minimized) value at $\kappa\approx 39$. Then x_3 (x_1) begins decreasing (increasing) till the proximity of the triple point $\kappa_{\rm tr}=37.4$, and for $\kappa<\kappa_{\rm tr}$, continues with the liquid-liquid phases in coexistence. Physically, the latter corresponds to a high density liquid x_2 (L_2' branch) substituting the solid phase x_3 (S_2' branch) and this L_2' coexists with the low density liquid x_1 (L_1 branch) which is the continuation of the original vapor phase (L_1' branch). These two cases delineate straightforwardly the fractional volume scenario which is less direct in the approach of match-solving Eqs. (6) and (8).

We turn next to another example. Figures 4(a)–4(d) show an anomaly in the phase diagrams of a suspension of monodisperse colloids induced by an extremely low concentration of electrolyte. Each colloid is ideally modeled to have a diameter $\sigma=625$ nm. The dispersions are limited to low macroion concentrations ($\eta_0<0.1$) and they are maintained at room temperature. Equation (10) has been used for calculating the liquid and solid f_i. We should emphasize a specific aspect of our numerical calculations. In the present case of very low salt concentrations, the determination of domains (single phase as well two phases in coexistence) by optimizing f_i is a straightforward procedure and numerically more stable than match-solving Eqs. (6)–(8) [17]. Let us examine Fig. 4(a). Each colloid carries a charge $Z=3500e$. Given the initial volume fractions in the range $0.005\lesssim\eta_0<0.082$, we find the system undergoing an unambiguous phase separation in two stages as the initial salt concentration $\rho_0^{(s)}$ is added. When $\rho_0^{(s)}$ is increased, the first stage exhibits a biphasic equilibrium between a vapor and a crystal (fcc) with the vapor phase $\rho_v^{(s)}$ spanning $0.75<\rho_v^{(s)}\lesssim 5.5$ μM, but on increasing $\rho_0^{(s)}$ further, the second stage makes an abrupt change to the liquid-crystal coexisting phases with the liquid phase $\rho_l^{(s)}$ assuming $5.5<\rho_l^{(s)}<6$ μM. When Z is reduced to $2700e$, one can see from Fig. 4(b) that there is a drastic shrinkage of the vapor-crystal domain with $\rho_v^{(s)}$ now restricted to values $0.6<\rho_v^{(s)}\lesssim 2.8$ μM. Away from the vapor-crystal domain, the system shifts over to the liquid-crystal

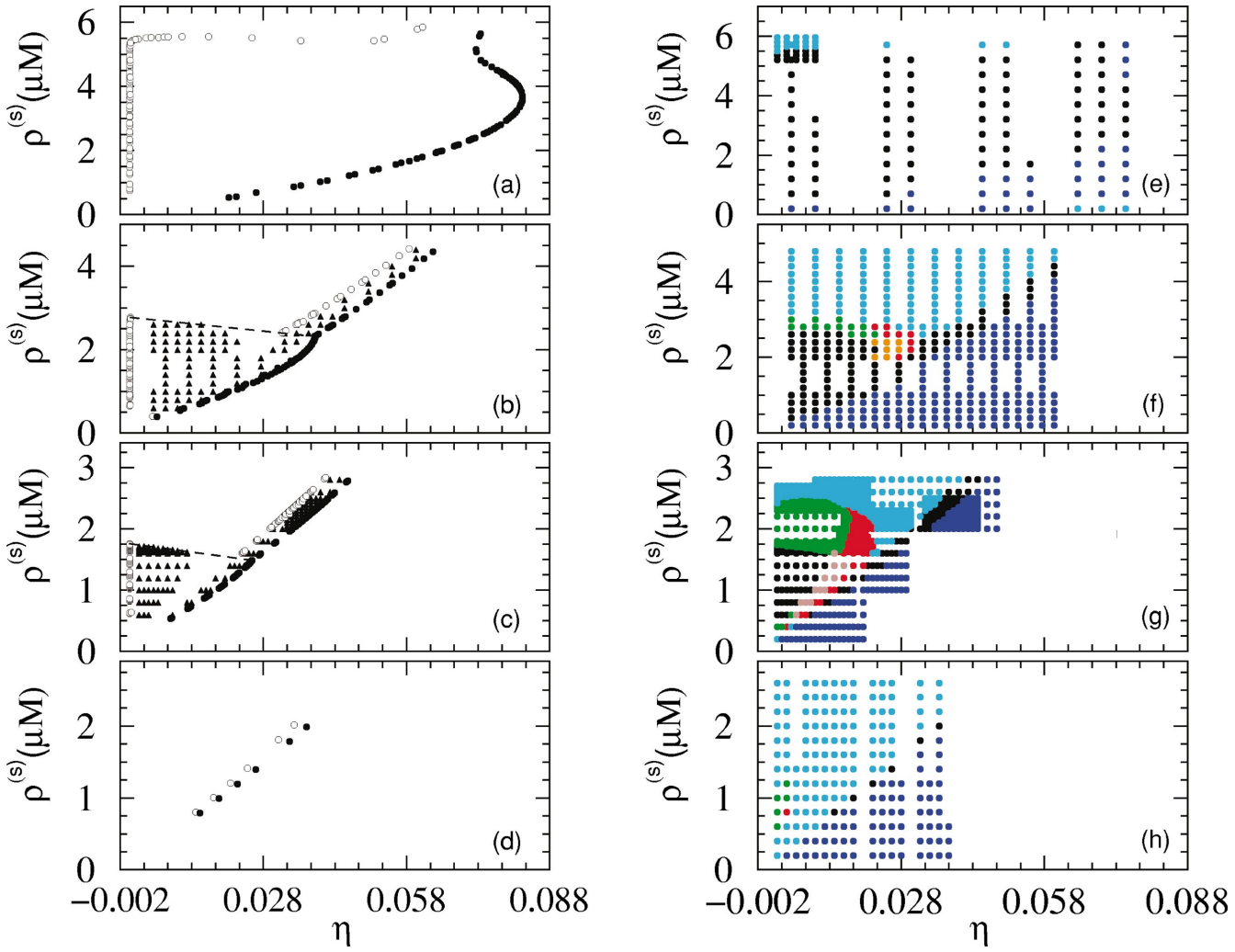

FIG. 4. (Color) Phase diagrams for electrolyte concentration $\rho^{(s)}$ vs colloidal packing fraction η. The left column (a)–(d) shows the boundaries of the vapor to low density liquid (open circles) coexisting with the (fcc) solid (solid circles). Solid triangles in (b) and (c) are coexisting phases and solid circles in (e)–(h) are either one phase or two coexisting phases. Notations for solid circles in the right column (e)–(h) are cyan, liquid; black, liquid-solid; blue, solid; green, liquid-liquid; orange, solid-solid; red, solid-liquid.

domain with the coexisting phases (solid triangles) confining to a limited region. These coexisting liquid and solid phases prolong thereon with $\rho_l^{(s)}$ reducing somewhat in magnitude ($2.4 < \rho_l^{(s)} \lesssim 4.5$ μM). Less amount of $\rho_0^{(s)}$ is needed for a vapor or a liquid to coexist with a crystal when the colloidal charge is smaller. At $Z=2515e$, the domain of the vapor-crystal coexisting phases (solid triangles) narrows still more as does the area between the liquid and crystal branches above the dashed line in Fig. 4(c). Thus, depending on the initial $\rho_0^{(s)}$ and η_0, the colloidal dispersion in this case phase separates into the coexisting phases of either a vapor and a crystal with $\rho_v^{(s)}=0.6-1.77$ μM or a liquid and a crystal with $\rho_l^{(s)}=1.6-2.82$ μM. At this value Z, the delimiting area of the vapor-crystal coexisting phases has been reduced substantially. Beyond a threshold value $Z_{\rm th}$ (lying somewhere in the range $2100e < Z_{\rm th} < 2515e$), keeping all other colloidal parameters unchanged, it is observed in Fig. 4(d) that the vapor-crystal transition disappears, and the phase transition is characterized wholly by the liquid-crystal transition. Notice that $\rho_l^{(s)}$ has by now been reduced to values much less than those at $Z=3500e$.

This anomalous "transition" of the phase diagrams $(\rho_0^{(s)}, \eta_0)$ raises three immediate questions. Why is it that on decreasing the charge $Z=3500e$ to a lower Z the vapor-crystal and liquid-crystal branches are restricted to narrower coexisting domains? What happens to those regions previously showing vapor-crystal and liquid-crystal phase separations? Since the vapor-crystal biphasic equilibrium vanishes at $Z=2100e$, would it be possible that other kinds of phase separations creep in because they are thermodynamically more favorable than the vapor-crystal and liquid-crystal transitions? We believe that the latter is a reasonable conjecture for the transition from the vapor-crystal to the liquid-crystal domain proceeds in an abrupt juxtaposition, and as shown in Figs. 4(b) and 4(c), the corresponding $\rho_v^{(s)}$ or $\rho_l^{(s)}$ has considerably diminished also. To delve deeper into these curious changes in phase diagrams, we appeal to f_m, studying the phase diagrams $(\rho_0^{(s)}, \eta_0)$ in quantitative detail. Figures

4(e)–4(h) summarize the equilibrium stable phases (homogeneous and coexisting) of charged colloidal dispersions obtained by optimizing f_m. The first striking feature we notice is indeed the emergence of several kinds of stable coexisting phases. In Fig. 4(f), for instance, f_m predicts the coexistence of a stable liquid-liquid domain within the region bounded by $0.006 < \eta_0 \lesssim 0.023$ and $2.6\ \mu\mathrm{M} \lesssim \rho_0^{(s)} \lesssim 3.0\ \mu\mathrm{M}$ (green solid circles), whereas for $0.023 \lesssim \eta_0 \lesssim 0.03$ and $2.0\ \mu\mathrm{M} \lesssim \rho_0^{(s)} < 2.9\ \mu\mathrm{M}$, the stable biphasic equilibrium is between the (low density) crystal and the (high density) liquid as well as between the (low density) crystal and the (high density) crystal. As Z is reduced to $2515e$, we obtain the growing predominance of the liquid-liquid and crystal-liquid biphasic domains. As shown in Fig. 4(g), these domains enlarge at the expense of the vapor-crystal and liquid-crystal domains. In particular, there is a tendency for the crystal-crystal and crystal-liquid coexisting phases to protrude downward, eroding the vapor-crystal domain in the region of low salt concentrations $\rho_0^{(s)}$. Perhaps more interesting is the scenario showing the seed of formation of the stable liquid-liquid phases near the low concentration region spanning between $0.004 \lesssim \eta_0 \lesssim 0.007$ and $0.4\ \mu\mathrm{M} \lesssim \rho_0^{(s)} \lesssim 0.6\ \mu\mathrm{M}$. Within the phase boundaries, the seeding of the coexisting liquid-liquid phases is seen to develop, and as Z decreases further, embraces the stable liquid-liquid domain on top [the shaded green in Fig. 4(g)]. Eventually, a stable loop boundary of the liquid-liquid domain appears at $Z = 2100e$ [Fig. 4(h)]. Note that there exists also a very small region of crystal-liquid coexisting phases. Consequently, the vapor-crystal biphasic domain at $Z = 3500e$ has been greatly substituted at $Z = 2100e$ by the homogeneous liquid, partly by the liquid-liquid, and non-negligibly by the crystal-liquid domain.

IV. CONCLUSION

Experimentally, the present method is appealing for f_m yields naturally the volume proportions pertaining to the coexisting subsystems that are ubiquitously observed [18] and have actually been measured [19] for charged colloidal systems. Theoretically, the present approach is sound for minimizing the Helmholtz free energy function is generally more efficient and numerically more stable than working with the pressure and chemical potential. This is especially so for charged colloids driven at very low ionic strength where the numerical root-finding procedure for solving Eqs. (6)–(8) is a delicate matter. Most importantly, the theory does not *per se* assume any phase coexisting with any other phase; the optimized f_m will tell the story, yielding either one homogenous phase or two phases in coexistence. In principle, the idea put forth here can be generalized to crosshatch the domains of coexisting multiphases which are rather tedious to determine numerically with an approach like solving Eqs. (6)–(8). We should perhaps note at this point that a quite similar line of thought has independently been advanced by Bodnár and Oosterbaan [19] and Renth *et al.* [20] in their studies of colloid-polymer mixtures.

To summarize, the calculated results given here reproduce many characteristics often obtained in the literature by match-solving Eqs. (6) and (8) for $\rho_0^{(s)} \gtrsim 1$ mM (e.g., Ref. [4]) or Eqs. (6)–(8) for $\rho_0^{(s)} \lesssim 1\ \mu$M (e.g., Ref. [5]). The present theory is certainly far more general strategically and, within the context of phase diagram study, has many attractive features. The theory yields naturally the *domains* of *single phase* as well as the *coexisting phases* together with their corresponding physical volume proportions. It can be generalized, in principle, to study the complex multiphases in coexistence such as the triphasic equilibrium of a polymer-colloid mixture reported experimentally [21]. Furthermore, our numerical results reveal clearly the role of an electrolyte in a charged colloidal suspension and exemplify its sensitivity to the electrostatic interactions between colloids. As demonstrated above for the two salt regimes, the present theory may serve as the paradigm for a variety of phase equilibrium phenomena in charged colloidal dispersions driven by electrolytes from the very low concentration regime ($\lesssim 1\ \mu$M), like those communicated recently by Roij *et al.* [5] and Warren [6] in phase diagram studies and Matsuoka *et al.* [11] in their observation of an anomalous structural transition, to electrolytes at moderate and high concentrations ($\gtrsim 1$ mM), as those reported by Sirota *et al.* [22] and us [4,23] in calculations of phase diagrams. Since the present approach starts with $(\rho_0^{(s)}, \rho_0)$ resembling closely the experimental condition, the idea put forth may be of great interest to experimentalists working in colloidal systems.

ACKNOWLEDGMENT

We acknowledge the financial support (Grant No. NSC92-2112-M-008-033) from the National Science Council, Taiwan, Republic of China.

[1] L. Mederos, J. Mol. Liq. **76**, 139 (1998).
[2] H. Löwen, Z. Phys. B: Condens. Matter **97**, 269 (1995); Physica A **235**, 129 (1997).
[3] S. K. Lai, W. P. Peng, and G. F. Wang, Phys. Rev. E **63**, 041511 (2001).
[4] S. K. Lai and K. L. Wu, Phys. Rev. E **66**, 041403 (2002).
[5] R. Van Roij, M. Dijkstra, and J. P. Hansen, Phys. Rev. E **59**, 2010 (1999).
[6] P. B. Warren, J. Chem. Phys. **112**, 4683 (2000).
[7] E. J. Verwey and J. G. Overbeek, *Theory of the Stability of Lyophobic Colloids* (Elsevier, Amsterdam, 1948).
[8] B. V. R. Tata and N. Ise, Phys. Rev. B **54**, 6050 (1996).
[9] C. N. Likos, Phys. Rep. **348**, 267 (2001).
[10] A. R. Denton, Phys. Rev. E **62**, 3855 (2000).
[11] H. Matsuoka, T. Harada, and H. Yamaoka, Langmuir **10**, 4423 (1994).
[12] H. Yoshida, J. Yamanaka, Tadanori Koga, Tsuyoshi Koga, N. Ise, and T. Hashimoto, Langmuir **15**, 2684 (1999).

[13] D. Ter Haar and H. Wergeland, *Element of Thermodynamics* (Addison-Wesley, Reading, MA, 1966).
[14] S. K. Lai, Phys. Rev. A **31**, 3886 (1985); **38**, 5707 (1988).
[15] W. Y. Shih, I. A. Aksay, and R. J. Kikuchi, J. Chem. Phys. **86**, 5127 (1987).
[16] S. K. Lai, Proc. Natl. Sci. Counc., Repub. China, Part A: Phys. Sci. Eng. **15**, 181 (1991); the density functional theory for an inhomogeneous distribution of particles is described at some length in this review article.
[17] Here the differentiations of the free energy density [Eqs. (6)–(8)] carried out to determine the boundaries of coexisting curves are rather sensitive and delicate. Roij *et al.* [5] (private communication) have in fact used a special trick to handle extremely small values. They have not described the numerical procedure in their paper, however.
[18] H. Yoshida, J. Yamanaka, T. Koga, N. Ise, and T. Hashimoto, Langmuir **14**, 569 (1998).
[19] I. Bodnár and W. D. Oosterbaan, J. Chem. Phys. **106**, 7777 (1997).
[20] F. Renth, W. C. K. Poon, and R. M. L. Evans, Phys. Rev. E **64**, 031402 (2001).
[21] R. M. L. Evans, W. C. K. Poon, and F. Renth, Phys. Rev. E **64**, 031403 (2001).
[22] E. B. Sirota, H. D. Ou-Yang, S. K. Sinha, P. M. Chaikin, J. D. Axe, and Y. Fujii, Phys. Rev. Lett. **62**, 1524 (1989).
[23] G. F. Wang and S. K. Lai, Phys. Rev. Lett. **82**, 3645 (1999).